1-1-2010

Multifunctional Magnetic-Optical Nanoparticle Probes for Simultaneous Detection, Separation, and Thermal Ablation of Multiple Pathogens

Chungang Wang
Purdue University - Main Campus

Joseph Irudayaraj
Purdue University - Main Campus, josephi@purdue.edu

small

Sensors

Multifunctional Magnetic–Optical Nanoparticle Probes for Simultaneous Detection, Separation, and Thermal Ablation of Multiple Pathogens

*Chungang Wang and Joseph Irudayaraj**

Multifunctional nanoparticles possessing magnetization and near-infrared (NIR) absorption have warranted interest due to their significant applications in magnetic resonance imaging, diagnosis, bioseparation, target delivery, and NIR photothermal ablation. Herein, the site-selective assembly of magnetic nanoparticles onto the ends or ends and sides of gold nanorods with different aspect ratios (ARs) to create multifunctional nanorods decorated with varying numbers of magnetic particles is described for the first time. The resulting hybrid nanoparticles are designated as Fe_3O_4–Au_{rod}–Fe_3O_4 *nanodumbbells and* Fe_3O_4–Au_{rod} *necklacelike constructs with tunable optical and magnetic properties, respectively. These hybrid nanomaterials can be used for multiplex detection and separation because of their tunable magnetic and plasmonic functionality. More specifically,* Fe_3O_4–Au_{rod} *necklacelike probes of different ARs are utilized for simultaneous optical detection based on their plasmon properties, magnetic separation, and photokilling of multiple pathogens from a single sample at one time. The combined functionalities of the synthesized probes will open up many exciting opportunities in dual imaging for targeted delivery and photothermal therapy.*

Keywords:
- gold
- magnetic materials
- nanorods
- pathogens
- sensors

1. Introduction

Multifunctional nanoparticles possessing magnetic properties and near-infrared (NIR) absorption have attracted a great deal of attention due to their prominence in magnetic resonance imaging (MRI), diagnosis, bioseparation, target delivery, and NIR photothermal ablation.[1] In addition to MRI[2] and separation, magnetic particles are also used for pathogen detection,[3] remote control of cellular behavior,[4] and targeted drug/gene delivery.[5] It is known that NIR-activated gold nanoparticles have been increasingly useful as labels for biosensing, contrast agents for various biomedical imaging methods, and photothermal therapy agents, in the form of gold nanoshells,[6] gold nanocages,[7] and gold nanorods (GNRs).[8] Advantages provided by GNRs over other nanostructures are: 1) their localized surface plasmon resonance (LSPR) tunability based on the aspect ratio (AR) from the visible to the NIR region;[8b,9] 2) the simple and established synthesis protocols for GNRs of various ARs;[8] and 3) GNRs are exceptionally good at absorbing NIR light and are very efficient in optothermal energy conversion, and hence are excellent photothermal therapy agents due to their higher absorption cross section at NIR frequencies per unit volume than most other nanostructures.[8b–d]

The combination of NIR optical and magnetic properties in a single nanocomposite can lead to the development of multitasking platforms for simultaneous biolabeling/imaging, cell sorting/separation, and photothermal therapy. More recent studies have combined the optical properties (NIR) of gold

[*] Prof. J. Irudayaraj, Dr. C. Wang
225 S. University Street
215 ABE Building
Birck Nanotechnology Center and Bindley Bioscience Center
Purdue University
West Lafayette, IN 47907 (USA)
E-mail: josephi@purdue.edu

Supporting Information is available on the WWW under http://www.small-journal.com or from the author.

DOI: 10.1002/smll.200901596

nanoshells with magnetic nanoparticles.[1] However, the reported nanoparticles suffer from either aggregation after gold coating or their larger size (>150 nm), which poses a limitation on targeted drug/gene delivery in living cells because of the size-dependent nature of the cellular uptake process.[10] The combination of GNRs and monodispersed magnetic nanoparticles can offset the aforementioned disadvantages due to the optical tunability of GNRs to detect multiple targets, strong NIR absorption capability for photokilling, and separation of targets through the magnetic properties of Fe_3O_4 nanoparticles.

Herein, we describe the development of a facile route to the site-selective assembly of Fe_3O_4 nanoparticles onto the ends or ends and sides of GNRs with different ARs to create multifunctional nanorods incorporating optical and magnetic materials that provide tunable plasmonic and magnetic properties. The resulting hybrid nanorods were designated as Fe_3O_4–Au_{rod}–Fe_3O_4 nanodumbbells (Fe_3O_4 spheres predominantly attached to the ends of GNRs) and Fe_3O_4–Au_{rod} necklacelike probes (several Fe_3O_4 nanoparticles functionalized around a GNR), respectively. The Fe_3O_4–Au_{rod} necklacelike hybrid nanorods of different ARs were then functionalized with relevant antibodies to construct efficient platforms for simultaneous optical detection, magnetic separation, and thermal ablation of multiple pathogens from a single sample.

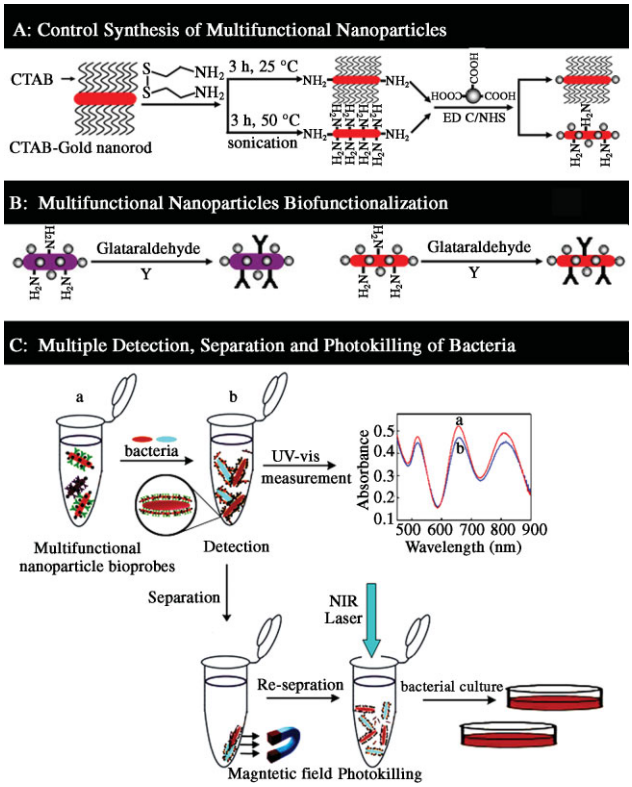

Scheme 1. A) Schematic showing the controlled assembly of Fe_3O_4 nanoparticles onto GNRs; B) biofunctionalization of multifunctional nanoparticles; and C) detection, separation, and thermal ablation of multiple bacterial targets. EDC: 1-ethyl-3-(3-dimethylaminopropyl) carbodiimide hydrochloride, NHS: *N*-hydroxysuccinimide.

2. Results and Discussion

2.1. Preparation of Fe_3O_4–Au_{rod}–Fe_3O_4 Nanodumbbells and Fe_3O_4–Au_{rod} Necklacelike Probes

GNRs with different ARs were prepared using a seed-mediated surfactant-directed approach previously reported by Nikoobakht and El-Sayed.[9a] Preferential binding of cetyltrimethylammonium bromide (CTAB) bilayers to the {100} facet of the longitudinal side of the GNRs left their ends ({111} facets) deprived of CTAB, which allowed selective binding of the thiol groups of cystamine dihydrochloride (abbreviated below to cystamine) to obtain partially activated GNRs decorated with free amine groups at room temperature. This preferential binding is probably due to the fact that the CTAB bilayer is less ordered at the ends than the sides of GNRs. To obtain fully activated GNRs with amine groups provided by cystamine self-assembled onto the ends ({111} facets) and sides ({100} facets) of the GNRs, the solution reaction temperature was elevated to result in the disassociation of CTAB from the {100} faces of the GNRs, thus leading to amine modification (Scheme 1A).

Monodispersed Fe_3O_4 nanoparticles capped with carboxyl groups were synthesized using a procedure described previously,[11] and the carboxyl-terminated Fe_3O_4 nanoparticles were selectively assembled onto the ends and sides of partially and completely amine-modified GNRs by 1-ethyl-3-(3-dimethylaminopropyl)carbodiimide hydrochloride/*N*-hydroxysuccinimide (EDC/NHS) chemistry to give hybrid multifunctional nanoparticles consisting of Fe_3O_4–Au_{rod}–Fe_3O_4 nanodumbbells and Fe_3O_4–Au_{rod} necklacelike probes (Scheme 1A). Two such batches of multifunctional probes were synthesized using GNRs of AR 2.0 and 3.4 to demonstrate multiplexing capabilities. Briefly, for the synthesis of Fe_3O_4–Au_{rod}–Fe_3O_4 nanodumbbells and Fe_3O_4–Au_{rod} necklacelike probes, a solution of NH_2-modified ends or ends and sides-modified GNRs was added to activated Fe_3O_4 nanoparticle solution enabled by EDC and NHS, respectively, and sonicated for 30 min (see the Experimental Section). The resulting solution was centrifuged at 4000 rpm and the unbound Fe_3O_4 nanoparticles were removed. After successful surface functionalization of GNRs to Fe_3O_4 nanoparticles to create Fe_3O_4–Au_{rod} necklacelike probes, the remaining amine groups of the GNRs could be subsequently used to attach protein molecules (for example, antibodies) with the glutaraldehyde (GA) protocol to construct multifunctional nanorod bioprobes (Scheme 1B). We investigated the use of multifunctional tunable nanosensors for rapid sensitive detection, magnetic separation, and thermal ablation of two key pathogenic food-borne bacteria, *Escherichia coli* and *Salmonella typhimurium* (Scheme 1C). In principle, the method presented here could be extended to detect, separate, and photokill multiple bacterial targets simultaneously because of the AR tenability of these multifunctional structures.

2.2. Characterization of Fe_3O_4–Au_{rod}–Fe_3O_4 Nanodumbbells and Fe_3O_4–Au_{rod} Necklacelike Probes

Figure 1A shows a transmission electron microscopy (TEM) image of monodispersed Fe_3O_4 nanoparticles with

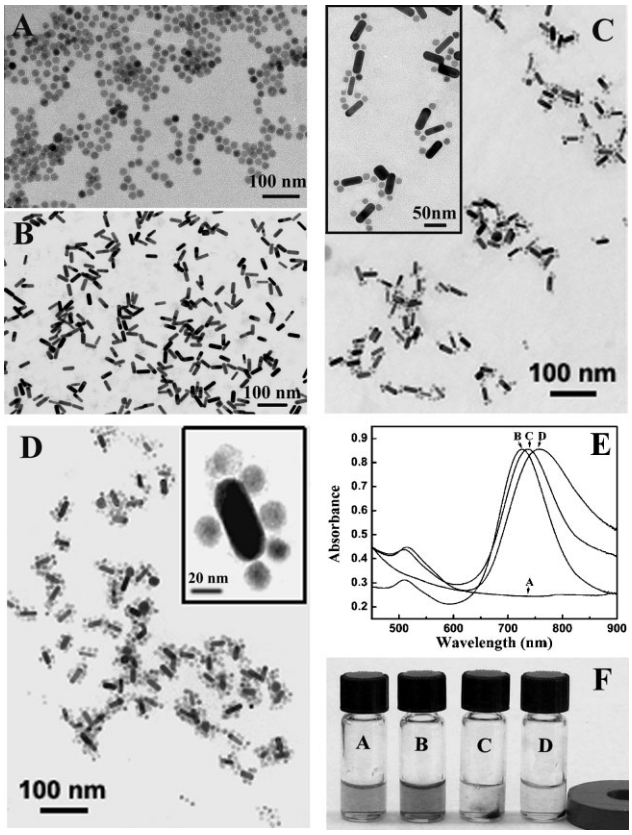

Figure 1. TEM images of A) COOH-modified Fe_3O_4 nanoparticles, B) NH_2-modified GNRs, C) Fe_3O_4 nanoparticles attached to the ends of GNRs (Fe_3O_4–Au_{rod}–Fe_3O_4 nanodumbbells), D) Fe_3O_4 nanoparticles assembled onto the ends and sides of GNRs (Fe_3O_4–Au_{rod} necklacelike probes), E) UV/Vis–NIR absorption spectra (A–D), and F) the corresponding samples.

carboxyl groups of size ≈15 nm. For site-selective assembly of carboxyl-terminated Fe_3O_4 nanoparticles to GNRs, we demonstrated a facile and novel method to partially and completely replace CTAB bilayers on GNRs modified with amine groups provided by a biocompatible and water-soluble chemical, cystamine, a disulfide-bearing compound with two amine groups that can easily self-assemble onto the gold surface via the Au–S bond.[12] The two different modification routes carried out were: undisturbed at room temperature, or under sonication at 50 °C for 3 h. The resulting GNRs with AR ≈ 3.4 and fully covered with amine groups appear very monodispersed, as shown in Figure 1B.

Carboxyl-terminated magnetic nanoparticles were assembled selectively onto the ends or ends and sides of GNRs with AR ≈ 3.4 modified by amine groups via EDC/NHS chemistry, as shown in Figure 1C and D. The resulting hybrid nanorods represent Fe_3O_4–Au_{rod}–Fe_3O_4 nanodumbbells and Fe_3O_4–Au_{rod} necklacelike probes, respectively. The distribution of the number of Fe_3O_4 nanoparticles attached per GNR is given in Figure S1 of the Supporting Information. About 60% of the Fe_3O_4–Au_{rod}–Fe_3O_4 nanodumbbells consists of two Fe_3O_4 particles.

Figure 1E (A–D) shows the respective UV/Vis–NIR spectra measured for carboxyl-functionalized Fe_3O_4 nanoparticles, amine-terminated GNRs, Fe_3O_4–Au_{rod}–Fe_3O_4 nanodumbbells, and Fe_3O_4–Au_{rod} necklacelike probes. The amine-modified GNRs have a weak transverse plasmon (TP) band at 524 nm and a strong longitudinal plasmon (LP) band at 732 nm (Figure 1E (B)). Obvious red shifts of 12 and 33 nm were observed to result in longitudinal peaks at 744 and 765 nm with a slight and an increased peak broadening for Fe_3O_4–Au_{rod}–Fe_3O_4 nanodumbbells and Fe_3O_4–Au_{rod} necklacelike probes, respectively (Figure 1E (C and D)), compared to amine-modified GNRs (Figure 1E (B)). This broadening effect reflects the variation of the local dielectric field when varying numbers of Fe_3O_4 nanoparticles are self-assembled onto GNRs activated either partially or completely by amine groups. The results presented show not only the controlled tunability of the plasmon properties by site-selective assembly of Fe_3O_4 nanoparticles onto GNRs, but also the fabrication of tunable magnetic probes produced by adjusting the number of Fe_3O_4 nanoparticles assembled onto GNRs. Figure 1F (A–D) shows photographs corresponding to the samples in Figure 1 E (A–D), which illustrate the effective separation of Fe_3O_4–Au_{rod}–Fe_3O_4 nanodumbbells and Fe_3O_4–Au_{rod} necklacelike constructs in the presence of a magnetic field (C and D). Fe_3O_4–Au_{rod} necklacelike probes are more easily separable by a magnet because the Fe_3O_4 nanoparticles decorate a higher surface area, while Fe_3O_4–Au_{rod}–Fe_3O_4 nanodumbbells respond weakly because of fewer Fe_3O_4 nanoparticles and increased CTAB bilayers on the {100} side facets.

The Fe_3O_4–Au_{rod}–Fe_3O_4 nanodumbbells and Fe_3O_4–Au_{rod} necklacelike probes are more readily perturbed upon exposure to a magnetic field than Fe_3O_4 nanoparticles because of the obvious clustering of particles as a unit. Once fabricated, the Fe_3O_4–Au_{rod}–Fe_3O_4 nanodumbbells, Fe_3O_4–Au_{rod} necklacelike probes, and unattached Fe_3O_4 nanoparticles can be separated from the stand-alone GNRs in the presence of a magnet. The free Fe_3O_4 nanoparticles are then removed by low-speed centrifugation. Additionally, a mixture of carboxyl-modified Fe_3O_4 nanoparticles and amine-terminated GNRs without the addition of EDC/NHS in the presence of a magnet was used as control. The result shows that no GNRs are attracted to the walls of the vial when a magnet is present, which indicates that Fe_3O_4 nanoparticles do not self-assemble onto the GNR surfaces (Supporting Information, Figure S2). The corresponding TEM image shown in Figure S3 demonstrates unattached Fe_3O_4 nanoparticles dispersed alongside GNRs in the mixture. Figure S4 shows photographs of Fe_3O_4–Au_{rod} necklacelike probes dispersed in water in the A) absence and B) presence of a magnet.

2.3. Biofunctionalized Fe_3O_4–Au_{rod} Necklacelike Probes

To impart biofunctionality, Fe_3O_4–Au_{rod}–Fe_3O_4 nanodumbbells and Fe_3O_4–Au_{rod} necklacelike probes were tethered to antibodies specific to target pathogens. Antibody attachment was facilitated by CTAB capping onto the sides of Fe_3O_4–Au_{rod}–Fe_3O_4 nanodumbbells to which an antibody or DNA could be attached through electrostatic attraction. The remaining unreactive amine groups on Fe_3O_4–Au_{rod} necklacelike probes were utilized to tether antibodies by covalent binding using the GA protocol. Briefly, Fe_3O_4–Au_{rod} necklacelike

probes (2 mL) with nanorod ARs ≈ 2.0 and 3.4 were dispersed in phosphate-buffered saline (PBS; 8.1 mmol L^{-1} Na_2HPO_4, 1.9 mmol L^{-1} NaH_2PO_4, 1.4 mol L^{-1} NaCl, 0.05% Tween-20, pH 7.4) containing 2% GA for about 1 h at room temperature. The hybrid nanoparticles were collected by centrifugation, redispersed in PBS, and then incubated with antibodies (*E. coli* and *S. typhimurium*). The antibody-modified Fe_3O_4–Au_{rod} hybrid nanorods were then washed with PBS to remove excess antibodies and kept at 4 °C in PBS.

The newly fabricated AR-tunable Fe_3O_4–Au_{rod} necklace-like probes were then used to detect two pathogens in a cocktail using a simple UV–visible spectrophotometer. The Supporting Information (Figure S5) shows Fe_3O_4–Au_{rod} necklacelike nanosensors fabricated with GNRs of AR ≈ 2.0.

2.4. Stability of Fe_3O_4–Au_{rod} Necklacelike Probes

The stability of Fe_3O_4–Au_{rod} necklacelike constructs was investigated by measuring their UV/Vis–NIR spectra in PBS (10 mM, pH 7.4) and ethanol. A slight change in the longitudinal and transverse peaks of the GNRs in PBS was observed compared to that in water, while an obvious red shift was observed in ethanol. The results show that the Fe_3O_4–Au_{rod} necklacelike probes in PBS and organic solvents (see the Supporting Information, inset in Figure S6) are stable and do not aggregate. In contrast, GNRs in solution unattached to Fe_3O_4 nanoparticles contribute to a change in color and precipitate in ethanol. A broadening of the LP band of bare GNRs was also noted, which indicates nanorod aggregation (see the Supporting Information, Figure S6). Our experiments demonstrate that Fe_3O_4 nanoparticles assemble onto GNRs and help minimize aggregation when the GNRs are suspended in ethanol.

2.5. Multiplex Pathogen Detection Using Fe_3O_4–Au_{rod} Necklacelike Probes

Recently, nanoparticle-based biosensors in the form of magnetic nanoparticles,[3] gold and silver nanoparticles,[13] fluorescent nanoparticles,[14] and Fe_3O_4/TiO_2 core/shell materials[15] have been used as either labels for detection and separation or as antibiotic agents for bacteria. But these methods have very limited ability to perform other functions in multiplexed detection, such as separation or thermal ablation of the captured pathogenic targets. We hypothesize that the fabricated Fe_3O_4–Au_{rod} probes with their magnetic and NIR absorption properties can serve as "multiplexers" for simultaneous detection, separation, and destruction of food-borne pathogens.

To demonstrate the utility of Fe_3O_4–Au_{rod} probes based on GNRs with different ARs in the above-mentioned applications, we developed *E. coli* and *S. typhimurium* antibody-conjugated Fe_3O_4–Au_{rod} sensors using GNRs with ARs ≈ 2.0 and 3.4, respectively. Figure 2 shows the spectra of a mixture of amine-modified GNRs with ARs ≈ 2.0 and 3.4, A) before and B) after the assembly of carboxyl-terminated Fe_3O_4 nanoparticles and C) upon further functionalization with antibodies targeting *E. coli* and *S. typhimurium*. The LP bands from the mixture of amine-functionalized GNRs show absorption peaks at 650

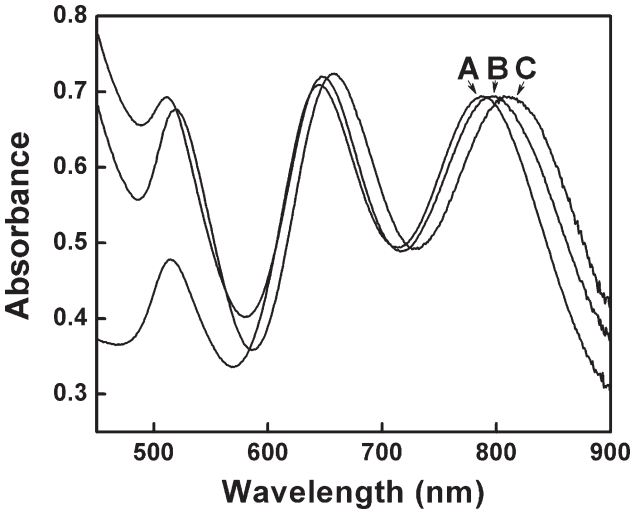

Figure 2. UV/Vis–NIR spectra of a mixture of GNRs of ARs ≈ 2.0 and 3.4, A) before and B) after modification by Fe_3O_4 nanoparticles, respectively, and C) after the attachment of *E. coli* and *S. typhimurium* antibodies.

(AR ≈ 2.0) and 780 nm (AR ≈ 3.4), as shown in Figure 2A. Red shifts of 6 and 15 nm in the LP band along with some peak broadening were observed corresponding to the two different ARs studied (Figure 2B), with the larger-AR GNRs responding to a greater extent to environmental changes than the smaller-AR nanorods. When anti-*E. coli* and anti-*S. typhimurium* antibodies were anchored to the Fe_3O_4–Au_{rod} sensors, the longitudinal peaks of the GNRs red-shifted to 671 and 815 nm and broadened (Figure 2C). This red shift could be attributed to an increase in the local refractive index due to the attachment of antibodies to the multifunctional probes.

Figure 3A shows the UV/Vis absorbance spectra obtained from samples that contained both *E. coli* and *S. typhimurium* at concentrations ranging from 1–10 to 10^5 cfu mL^{-1} (colony-forming units per mL) after 30 min of incubation with the sensors. As seen from the spectra, the intensity of the LP bands of the two Fe_3O_4–Au_{rod} sensors absorbing at the different wavelengths decreased from that of the control. The results indicate that the Fe_3O_4–Au_{rod} sensors based on GNRs with the two ARs could bind to their own target bacteria in a mixture of the species, thus resulting in an intensity decrease of the respective LP band. This is because the *E. coli* and *S. typhimurium* are much larger in size (≈1–3 μm) than the Fe_3O_4–Au_{rod} necklacelike probes (≈80 nm) and several of the Fe_3O_4–Au_{rod} probes can attach to a single bacterium. It is worth noting that the LP bands only decreased in intensity after the recognition event, that is, binding of anti-*E. coli*- and anti-*S. typhimurium*-conjugated probes to *E. coli* and *S. typhimurium*. The decrease in intensity of the LP bands at different concentrations (1–10 to 10^5 cfu mL^{-1}) is most likely due to the binding of Fe_3O_4–Au_{rod} sensors to *E. coli* and *S. typhimurium* surfaces. The results indicate that the detection of *E. coli* and *S. typhimurium* at low concentrations, that is, less than 10^2 cfu mL^{-1}, can be realized in less than 30 min. The detection method demonstrated is very rapid and simple, since a reduction in intensity of the LP bands of Fe_3O_4–Au_{rod} probes can be monitored by a simple UV/Vis optical readout. A critical

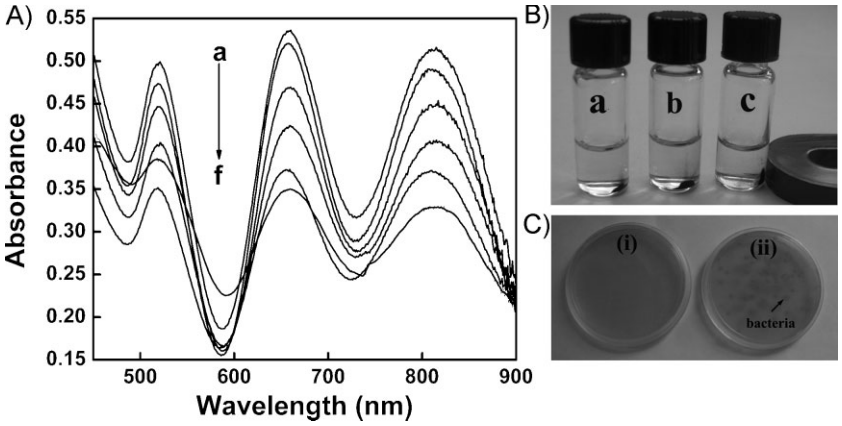

Figure 3. A) UV/Vis–NIR absorbance spectra of anti-*E. coli*- and anti-*S. typhimurium*-conjugated Fe_3O_4–Au_{rod} necklacelike probes based on GNRs with ARs ≈ 2.0 and 3.4, a) before and b–f) after the addition of *E. coli* and *S. typhimurium*, respectively, at concentrations of 1–10, 10^2, 10^3, 10^4, and 10^5 cfu mL^{-1}. B) Fe_3O_4–Au_{rod} necklacelike probes based on GNRs with ARs ≈ 2.0 (a) and 3.4 (b) modified with antibodies for *E. coli* and *S. typhimurium*, respectively, in the presence of a magnet, and c) anti-*E. coli*- and anti-*S. typhimurium*-functionalized Fe_3O_4–Au_{rod} necklacelike probes in a mixture of *E. coli* and *S. typhimurium*, with the aid of a magnet. C) *E. coli* and *S. typhimurium* cultures upon incubation. Here, (i) and (ii) denote antibody-modified and bare Fe_3O_4–Au_{rod} necklacelike probes of ARs ≈ 2.0 and 3.4 targeted for *E. coli* and *S. typhimurium*, respectively, in PBS after irradiation by NIR light (785 nm) for 15 min at 50 mW prior to cell culturing.

problem when detecting large numbers of targets simultaneously is the binding specificity. A high degree of specificity between antibodies and the corresponding bacteria was confirmed in our previous work,[16] consistent with other studies.[14]

Observations of LP band changes can be further confirmed by TEM. Figure 4A presents the TEM image of bacteria bound to antibody-functionalized Fe_3O_4–Au_{rod} necklacelike sensors after a magnetic separation step. The cell walls of the bacteria trapped by the Fe_3O_4–Au_{rod} necklacelike probes are covered with nanoparticles, thus confirming that the multifunctional probes have the capacity to target and separate pathogens with a good specificity as defined by the target antibodies.

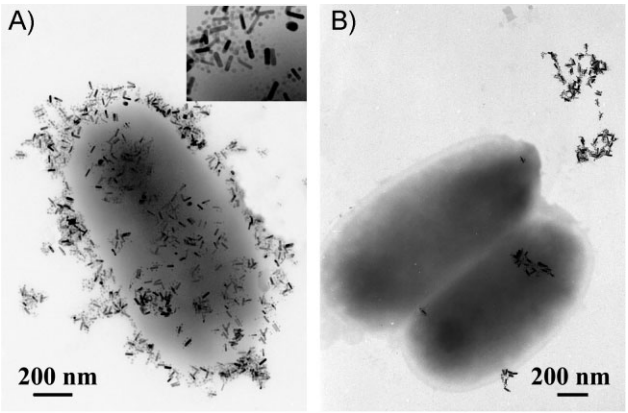

Figure 4. TEM images showing A) antibody-conjugated Fe_3O_4–Au_{rod} necklacelike probes bound to bacteria and B) nonspecific binding of bare Fe_3O_4–Au_{rod} necklacelike probes to bacteria. The inset in (A) shows a high-magnification image of Fe_3O_4–Au_{rod} necklacelike probes bound to a bacterium surface.

Some nonspecific binding was observed (Figure 4B); however, this affects detection only negligibly.

2.6. Separation of Multiple Pathogens Based on Fe_3O_4–Au_{rod} Necklacelike Probes

Figure 3B shows photographs of Fe_3O_4–Au_{rod} necklacelike probes based on GNRs with ARs of a) ≈2.0 and b) 3.4 in the presence of a magnet, and c) a mixture of two Fe_3O_4–Au_{rod} necklacelike probes after a recognition and magnetic separation event. As seen from the photographs, multiple bacterial targets can be separated from the solution using the Fe_3O_4–Au_{rod} sensors with GNRs of different ARs.

2.7. Thermal Ablation of Multiple Pathogens Based on Fe_3O_4–Au_{rod} Necklacelike Probes

To demonstrate the thermal ablation property, two Fe_3O_4–Au_{rod} necklacelike probes were allowed to interact with their target bacteria (*E. coli* and *S. typhimurium*) for 30 min, and the probe-bound cells were magnetically separated. Fe_3O_4–Au_{rod} bacteria-bound conjugates were then resuspended in PBS solution and irradiated with NIR light (785 nm) at 50 mW for 15 min. The resulting conjugates were then separated and diluted, and cultured on a Luria–Bertani (LB) plate for 17 h at 37 °C (see the Experimental Section) to assess viability. Figure 3C shows the growth of *E. coli* and *S. typhimurium* incubated in PBS buffer, when unmodified probes were used as a control alongside targeted Fe_3O_4–Au_{rod} sensors. After NIR radiation, it was clear from Figure 3C (i) that microorganisms did not grow, while the culture plate with unmodified probes did not have enough Fe_3O_4–Au_{rod} sensors (Figure 4B shows fewer probes bound to the pathogen when not targeted) to target and kill the pathogens. Consequently, a number of bacterial colonies could be seen (Figure 4B) even after NIR irradiation (Figure 3C (ii)). The results indicate that the Fe_3O_4–Au_{rod} necklacelike probes based on GNRs with different ARs anchor onto the bacterial surface (Figure 4A shows a very high probe density when targeted) and absorb sufficient energy upon excitation in the NIR region to kill the target pathogens.

3. Conclusions

In summary, we have demonstrated for the first time the site-selective and tunable assembly of Fe_3O_4 nanoparticles onto GNRs of different ARs to construct multifunctional Fe_3O_4–Au_{rod}–Fe_3O_4 nanodumbbells and Fe_3O_4–Au_{rod} necklacelike probes with tunable plasmonic and magnetic properties. The fabricated Fe_3O_4–Au_{rod} necklacelike probes were then used for the simultaneous detection of multiple pathogens in a single sample, based on plasmon absorbance, magnetic separation, and thermal ablation. We expect the newly

synthesized tunable nanoprobes with their multifunctional properties to open many exciting opportunities in diagnostics, therapy, and as in vivo contrast agents.

4. Experimental Section

Synthesis of COOH-functionalized magnetic nanoparticles: Uniform 15-nm magnetic nanoparticles capped with oleic acid were synthesized by a previously reported procedure.[11a] The surfaces of the magnetic nanoparticles were functionalized with COOH groups by coating with amphiphilic polymers.[11b],c

Synthesis of GNRs with different ARs: CTAB-stabilized GNRs were synthesized using the seed-mediated growth method improved by El-Sayed and co-workers. [9a] Briefly, the seed solution was prepared by mixing CTAB (0.2 M, 5 mL) and $HAuCl_4$ (0.5 mM, 5 mL) with freshly prepared ice-cold $NaBH_4$ (10 mM, 0.6 mL). After 5 h, the seed solution was used for the synthesis of GNRs. In two flasks, CTAB (0.2 M, 50.0 mL) was mixed with silver nitrate (10 mM, 30 and 120 μL, respectively) and $HAuCl_4$ (1 mM, 50.0 mL). After gently mixing the solution, ascorbic acid (0.10 M, 600 μL) was added. Then the seed solution (120 μL) was finally added to the mixtures to initiate growth to yield GNRs of ARs ≈ 2.0 and 3.4, respectively. Excess CTAB was removed by centrifuging twice at 8000 rpm, the supernatant was discarded, and the particles were redispersed in pure water.

Selective modification of GNRs with NH_2 groups: a) NH_2 modification of the ends of GNRs was carried out in a calculated volume of cystamine (0.01 M) with the as-prepared GNR solution to give a cystamine concentration of 100 μM. The resulting solution was kept at room temperature for 3 h. b) Preferential NH_2 modification of the ends and sides of GNRs was achieved as follows. An aqueous solution of cystamine (20 mM, 0.5 mL) was added to a GNR solution (5 mL), and the mixture was centrifuged once and sonicated for 3 h at 50 °C. The resulting GNRs were then collected by centrifugation twice at 7000 rpm for 15 min and the excess cystamine and CTAB were removed. The material was resuspended in a CTAB solution (0.005 M) to yield a final concentration of 100 nM.

Selective assembly of magnetic nanoparticles to NH_2-modified GNRs: A solution of (Fe)COOH-modified Fe_3O_4 nanoparticles (0.1 mL, 5 mg mL^{-1}) was added to borate buffer (10 mM, 1 mL, pH 5.5). Then EDC (100 μL, 1 mg mL^{-1}) and NHS (50 μL, 1 mg mL^{-1}) were added to the Fe_3O_4 nanoparticle solution and the mixture was sonicated at 4 °C for 15 min. Excess EDC and NHS were removed by centrifugation at 14 000 rpm for 10 min. Briefly, to synthesize Fe_3O_4–Au_{rod}–Fe_3O_4 nanodumbbells and Fe_3O_4–Au_{rod} necklacelike probes, a solution (3 mL) of NH_2-modified ends or ends and sides-modified GNRs was added to activated Fe_3O_4 nanoparticle solution (3 or 10 μL) enabled by EDC and NHS, respectively, and the mixture was sonicated for 30 min. The resulting solution was then centrifuged at 4000 rpm to remove unbound Fe_3O_4 nanoparticles. Subsequently, free GNRs unattached to Fe_3O_4 nanoparticles were separated in the presence of an external magnetic field.

Biofunctionalization of Fe_3O_4–Au_{rod} necklacelike probes with antibodies: Fe_3O_4–Au_{rod} necklacelike probes with some of the remaining NH_2 groups were dispersed in PBS (8.1 mmol L^{-1} Na_2HPO_4, 1.9 mmol L^{-1} NaH_2PO_4, 1.4 mol L^{-1} NaCl, 0.05% Tween-20, pH 7.4) containing 2% GA for about 1 h at room temperature. The hybrid nanoparticles were collected by centrifugation, redispersed in PBS, and then incubated with antibodies purchased from Fisher Scientific (Pittsburgh, PA) for 3 h at 37 °C. The antibody-modified Fe_3O_4–Au_{rod} hybrid nanorods were then washed with PBS to remove excess antibodies and kept at 4 °C in PBS.

Preparation of bacterial samples: Bacteria (*E. coli* and *S. typhimurium*) were grown in LB broth at 37 °C and collected with sterile plastic inoculating loops from solid culture plates; the samples were collected after the bacteria were cultured for 13 h. The collected samples were then added to PBS (3 mL, pH 7.4) and the mixture was vortexed, centrifuged for 10 min at 5800 rpm, and the supernatant was discarded. This procedure was repeated three times.

Optical detection of multiple bacterial targets: Fe_3O_4–Au_{rod} necklacelike bioprobes with GNRs of ARs 2.0 and 3.4 were conjugated with antibodies for *E. coli* and *S. typhimurium* and dispersed in PBS (1 mL). *E. coli* and *S. typhimurium* cells were introduced in varying concentrations, the mixture was gently shaken at room temperature for 30 min, and the absorbance was measured using a Jasco V570 UV/Vis–NIR spectrometer (Jasco, Inc., Easton, MD).

Separation of multiple bacterial targets: Fe_3O_4–Au_{rod} sensor-bound bacteria (*E. coli* O157:H7 and *S. typhimurium*) were separated from the solution by an external magnetic field.

Photokilling of multiple bacterial targets: The antibody-conjugated Fe_3O_4–Au_{rod} necklacelike sensors (500 μL) were vortexed for 30 min with *E. coli* and *S. typhimurium* at a concentration of 10^5 cfu mL^{-1}. The nanoparticle–bacteria conjugates were isolated by magnetic separation, rinsed with PBS, and then resuspended and irradiated with a 785 nm laser for 15 min. After irradiation, the suspension was diluted prior to culturing on a LB plate to show cell viability.

Acknowledgements

This research was supported by the ARS-USDA and Purdue Center for Food Safety Engineering Grant (1935-42000-035). Sandeep Ravindranath is acknowledged for his assistance in culturing of bacteria. Magnetic particles were provided partly by A. Wang from Ocean Nanotech LLC., Springdale, AR, http://www.oceannanotech.com/. This research was carried out at the Physiological Sensing Facility of the Bindley Bioscience Center.

[1] a) J. Kim, S. Park, J. E. Lee, S. M. Jin, J. H. Lee, I. S. Lee, I. Yang, J. S. Kim, S. K. Kim, M. H. Cho, T. Hyeon, *Angew. Chem.* **2006**, *118*, 7918; *Angew. Chem. Int. Ed.* **2006**, *45*, 7754; b) V. Salgueirino-Maceira, M. A. Correa-Duarte, M. Farle, A. Lopez-Quintela, K. Sieradzki, R. Diaz, *Chem. Mater.* **2006**, *18*, 2701; c) X. J. Ji, R. P. Shao, A. M. Elliott, R. J. Stafford, E. Esparza-Coss, J. A. Bankson, G. Liang, Z. P. Luo, K. Park, J. T. Markert, C. Li, *J. Phys. Chem. C* **2007**, *111*, 6245; d) T. A. Larson, J. Bankson, J. Aaron, K. Sokolov, *Nanotechnology* **2007**, *18*, 325101; e) L. Y. Wang, J. W. Bai, Y. J. Li, Y. Huang, *Angew. Chem.* **2008**, *120*, 2473. *Angew. Chem. Int. Ed.* **2008**, *47*, 2439;

f) H. Park, J. Yang, S. Seo, K. Kim, J. Suh, D. Kim, S. Haam, K. H. Yoo, *Small* **2008**, *4*, 192.

[2] a) W. S. Seo, J. H. Lee, X. M. Sun, Y. Suzuki, D. Mann, Z. Liu, M. Terashima, P. C. Yang, M. V. McConnell, D. G. Nishimura, H. J. Dai, *Nat. Mater.* **2006**, *5*, 971; b) M. Lewin, N. Carlesso, C. H. Tung, X. W. Tang, D. Cory, D. T. Scadden, R. Weissleder, *Nat. Biotechnol.* **2000**, *18*, 410; c) Y. Jun, Y.-M. Huh, J. Choi, J.-H. Lee, H.-T. Song, S. Kim, S. Yoon, K.-S. Kim, J.-S. Shin, J.-S. Suh, J. Cheon, *J. Am. Chem. Soc.* **2005**, *127*, 5732; d) Y.-M. Huh, Y. Jun, H.-T. Song, S. Kim, J. Choi, J.-H. Lee, S. Yoon, K.-S. Kim, J.-S. Shin, J.-S. Suh, J. Cheon, *J. Am. Chem. Soc.* **2005**, *127*, 12387; e) J.-H. Lee, Y.-M. Huh, Y. Jun, J. Seo, J. Jang, H.-T. Song, S. Kim, E.-J. Cho, H.-G. Yoon, J.-S. Suh, J. Cheon, *Nat. Med.* **2007**, *13*, 95; f) F. Q. Hu, L. Wei, Z. Zhou, Y. L. Ran, Z. Li, M. Y. Gao, *Adv. Mater.* **2006**, *18*, 2553.

[3] a) J. Gao, L. Li, P.-L. Ho, G. C. Mak, H. Gu, B. Xu, *Adv. Mater.* **2006**, *18*, 3145; b) H. Gu, P.-L. Ho, K. W. T. Tsang, L. Wang, B. Xu, *J. Am. Chem. Soc.* **2003**, *125*, 15702; c) H. W. Gu, K. M. Xu, C. J. Xu, B. Xu, *Chem. Commun.* **2006**, 941; d) Y.-S. Lin, P.-J. Tsai, M.-F. Weng, Y.-C. Chen, *Anal. Chem.* **2005**, *77*, 1753; e) K. El-Boubbou, C. Gruden, X. F. Huang, *J. Am. Chem. Soc.* **2007**, *129*, 13392.

[4] a) R. J. Mannix, S. Kumar, F. Cassiola, M. Montoya-Zavala, D. E. Ingber, *Nat. Nanotechnol.* **2008**, *3*, 36; b) J. Dobson, *Nat. Nanotechnol.* **2008**, *3*, 139.

[5] a) J. R. McCarthy, K. A. Kelly, E. Y. Sun, R. Weissleder, *Nanomedicine* **2007**, *2*, 153; b) Z. Medarova, W. Pham, C. Farrar, V. Petkova, A. Moore, *Nat. Med.* **2007**, *13*, 372; c) S. Giri, B. G. Trewyn, M. P. Stellmaker, V. S. Y. Lin, *Angew. Chem.* **2005**, *117*, 5166; *Angew. Chem. Int. Ed.* **2005**, *44*, 5038; d) T. J. Yoon, J. S. Kim, B. G. Kim, K. N. Yu, M. H. Cho, J. K. Lee, *Angew. Chem.* **2005**, *117*, 1092; *Angew. Chem. Int. Ed.* **2005**, *44*, 1068; e) Y.-M. Huh, E.-S. Lee, J.-H. Lee, Y.-W. Jun, P.-H. Kim, C.-O. Yun, J.-H. Kim, J. S. Suh, J. Cheon, *Adv. Mater.* **2007**, *19*, 3109; f) B. F. Pan, D. X. Cui, Y. Sheng, C. G. Ozkan, F. Gao, R. He, Q. Li, P. Xu, T. Huang, *Cancer Res.* **2007**, *67*, 8156.

[6] a) L. R. Hirsch, R. J. Stafford, J. A. Bankson, S. R. Sershen, B. Rivera, R. E. Price, J. D. Hazle, N. J. Halas, J. L. West, *Proc. Natl. Acad. Sci. USA* **2003**, *100*, 13549; b) C. Loo, A. Lowery, N. J. Halas, J. L. West, R. A. Drezek, *Nano Lett.* **2005**, *5*, 709; c) A. M. Gobin, M. H. Lee, N. J. Halas, W. D. James, R. A. Drezek, J. L. West, *Nano Lett.* **2007**, *7*, 1929; d) J. Chen, F. Saeki, B. J. Wiley, H. Chang, M. J. Cobb, Z.-Y. Li, L. Au, H. Zhang, M. B. Kimmey, X. Li, Y. Xia, *Nano Lett.* **2005**, *5*, 473.

[7] a) J. Y. Chen, D. L. Wang, J. F. Xi, L. Au, A. Siekkinen, A. Warsen, Z. Y. Li, H. Zhang, Y. N. Xia, X. D. Li, *Nano Lett.* **2007**, *7*, 1318; b) J. Y. Chen, B. Wiley, Z. Y. Li, D. Campbell, F. Saeki, H. Cang, L. Au, J. Lee, X. D. Li, Y. N. Xia, *Adv. Mater.* **2005**, *17*, 2255; c) S. E. Skrabalak, J. Y. Chen, L. Au, X. M. Lu, X. D. Li, Y. N. Xia, *Adv. Mater.* **2007**, *19*, 3177.

[8] a) C. C. Chen, Y. P. Lin, C. W. Wang, H. C. Tzeng, C. H. Wu, Y. C. Chen, C. P. Chen, L. C. Chen, Y. C. Wu, *J. Am. Chem. Soc.* **2006**, *128*, 3709; b) X. H. Huang, I. H. El-Sayed, W. Qian, M. A. El-Sayed, *J. Am. Chem. Soc.* **2006**, *128*, 2115; c) R. S. Norman, J. W. Stone, A. Gole, C. J. Murphy, T. L. Sabo-Attwood, *Nano Lett.* **2008**, *8*, 302; d) D. Pissuwan, S. M. Valenzuela, C. M. Miller, M. B. Cortie, *Nano Lett.* **2007**, *7*, 3808; e) T. B. Huff, L. Tong, Y. Zhao, M. N. Hansen, J. X. Cheng, A. Wei, *Nanomedicine* **2007**, *2*, 125; f) C. G. Wang, Z. F. Ma, T. T. Wang, Z. M. Su, *Adv. Funct. Mater.* **2006**, *16*, 1673; g) C. X. Yu, H. Nakshatri, J. Irudayaraj, *Nano Lett.* **2007**, *7*, 2300; h) C. G. Wang, Y. Chen, T. T. Wang, Z. F. Ma, Z. M. Su, *Adv. Funct. Mater.* **2008**, *18*, 355; i) C. X. Yu, J. Irudayaraj, *Anal. Chem.* **2007**, *79*, 572; j) L. Tong, Y. Zhao, T. B. Huff, M. N. Hansen, A. Wei, J. X. Cheng, *Adv. Mater.* **2007**, *19*, 3136; k) C. G. Wang, Y. Chen, T. T. Wang, Z. F. Ma, Z. M. Su, *Chem. Mater.* **2007**, *19*, 5809; l) K. M. Mayer, S. Lee, H. W. Liao, B. C. Rostro, A. Fuentes, P. T. Scully, C. L. Nehl, J. H. Hafner, *ACS Nano* **2008**, *2*, 687.

[9] a) B. Nikoobakht, M. A. El-Sayed, *Chem. Mater.* **2003**, *15*, 1957; b) L. F. Gou, C. J. Murphy, *Chem. Mater.* **2005**, *17*, 3668.

[10] W. Jiang, B. Y. S. Kim, J. T. Rutka, W. C. W. Chan, *Nat. Nanotechnol.* **2008**, *3*, 145.

[11] a) W. W. Yu, J. C. Falkner, C. T. Yavuz, V. L. Colvin, *Chem. Commun.* **2004**, 2306; b) C. J. Lin, R. A. Sperling, J. K. Li, T. Y. Yang, P. Y. Li, M. Zanella, W. H. Chang, W. J. Parak, *Small* **2008**, *4*, 334; c) X. H. Gao, Y. Cui, R. M. Levenson, L. W. K. Chung, S. M. Nie, *Nat. Biotechnol.* **2004**, *22*, 969.

[12] a) X. S. Kou, S. Z. Zhang, Z. Yang, C. K. Tsung, G. D. Stucky, L. D. Sun, J. F. Wang, C. H. Yan, *J. Am. Chem. Soc.* **2007**, *129*, 6402; b) Z. H. Nie, D. Fava, E. Kumacheva, S. Zou, G. C. Walker, M. Rubinstein, *Nat. Mater.* **2007**, *6*, 609; c) P. K. Sudeep, S. T. S. Joseph, K. G. Thomas, *J. Am. Chem. Soc.* **2005**, *127*, 6516; d) J. Y. Chang, H. M. Wu, H. Chen, Y. C. Ling, W. H. Tan, *Chem. Commun.* **2005**, 1092.

[13] a) J. Gil-Tomas, S. Tubby, I. P. Parkin, N. Narband, L. Dekker, S. P. Nair, M. Wilson, C. Street, *J. Mater. Chem.* **2007**, *17*, 3739; b) W.-C. Huang, P.-J. Tsai, Y.-C. Chen, *Nanomedicine* **2007**, *2*, 777; c) G. Naja, P. Bouvrette, S. Hrapovic, J. H. T. Luong, *Analyst* **2007**, *132*, 679; d) S. A. Kalele, A. A. Kundu, S. W. Gosavi, D. N. Deobagkar, D. D. Deobagkar, S. K. Kulkarni, *Small* **2006**, *2*, 335.

[14] a) L. Wang, W. J. Zhao, M. B. O'Donoghue, W. H. Tan, *Bioconjugate Chem.* **2007**, *18*, 297; b) L. Yang, Y. B. Li, *Analyst* **2006**, *131*, 394.

[15] W. J. Chen, P. J. Tsai, Y. C. Chen, *Small* **2008**, *4*, 485.

[16] C. G. Wang, J. Irudayaraj, *Small* **2008**, *4*, 2204.

Received: August 25, 2009
Published online: November 26, 2009

